Journal of Hydrology: Regional Studies 44 (2022) 101275

Contents lists available at ScienceDirect

Journal of Hydrology: Regional Studies

journal homepage: www.elsevier.com/locate/ejrh

Improvement of evapotranspiration estimates for grasslands in the southern Great Plains: Comparing a biophysical model (SWAT) and remote sensing (MODIS)

Lei Qiao [a,*], Rodney Will [b], Kevin Wagner [a,c], Tian Zhang [b], Chris Zou [b,*]

[a] Oklahoma Water Resources Center, Oklahoma State University, Stillwater, OK 74078, USA
[b] Department of Natural Resource Ecology and Management, Oklahoma State University, Stillwater, OK 74078, USA
[c] Department of Plant and Soil Sciences, Oklahoma State University, Stillwater, OK 74078, USA

ARTICLE INFO

Keywords:
Water Resources
Southern Great Plains
Vegetation productivity
SWAT
MODIS

ABSTRACT

Study region: Mixed- and tall-grass prairies in the southern Great Plains, USA
Study focus: Estimates of evapotranspiration (ET) are widely available from remote sensing and commonly used for water management. However, this approach is limited by prolonged satellite revisit periods and prominent algorithm-induced bias. We compared ET estimates from MODIS (Moderate Resolution Imaging Spectroradiometer) products and those based on the biophysically-based Soil and Water Assessment Tool (SWAT) to measurements using the eddy covariance (EC) technique for a subhumid, tall-grass prairie site near Stillwater, Oklahoma (OK) and a semiarid, mixed-grass prairie site near Clinton, OK in the southern Great Plains, USA.
New hydrological insights for the region: SWAT and MODIS produced ET estimates closer to EC measurements for the tall-grass prairie (calibration site) than for the mixed-grass prairie (validation site), with a better performance from SWAT. For the tall-grass prairie, the R^2 values were relatively high and comparable (0.77 and 0.87), and the biases were relatively small (-0.40% and 5.04%) for the SWAT and MODIS comparisons to EC. SWAT performed much better than MODIS for the mixed-grass prairie with R^2 values of 0.68 vs. 0.13 and bias of − 1.87% vs. − 45.71%, respectively. The SWAT simulation also reproduced better estimates of aboveground net primary productivity than the MODIS products. This study suggests that site-specific SWAT simulations can produce better ET estimates than MODIS products, especially in the water-limited mixed-grass prairie.

1. Introduction

Evapotranspiration (ET), the loss of water to the atmosphere through evaporation and transpiration, is essentially a passive response of ecosystems to climate, soil moisture, and vegetation. Grass-dominated ecosystems, such as the prairies, represent a major land cover type globally and provide essential ecosystem services such as clean water, forage, wildlife habitat, and drought and flood mitigation (Diego et al., 2016; Lu et al., 2011; Norris et al., 2001; Van Auken, 2000; Weltz et al., 2011). Most grass-dominated ecosystems are in water-limited environments where water availability is central to the ecosystem services provided. It is imperative to

Abbreviations: SWAT, Soil and Water Assessment Tool; MODIS, Moderate Resolution Imaging Spectroradiometer.

* Corresponding authors.
E-mail addresses: lei.qiao@okstate.edu (L. Qiao), chris.zou@okstate.edu (C. Zou).

https://doi.org/10.1016/j.ejrh.2022.101275
Received 4 May 2022; Received in revised form 15 November 2022; Accepted 19 November 2022
Available online 23 November 2022

improve ET estimates to support effective water resource management and decision-making for water security and ecosystem sustainability in these systems.

Studies estimating ET dynamics for grass-dominated ecosystems have used different approaches (e.g., Kurc and Small, 2007; Scott et al., 2006a and 2006b; Yepez et al., 2005). Canopy chamber and lysimetric methods have been used for ET measurement at the plot scale (Alfieri et al., 2009; Johnson et al., 2003; Todd et al., 2000; Kurc et al., 2004). Although relatively accurate, these methods are unable to provide the needed data for water resources management and conservation practice implementation at larger ecosystem or landscape scales. Currently, eddy covariance (EC) and remote sensing are two common techniques to estimate ET at the ecosystem scale. The EC method is the most direct approach for measuring vertical water and carbon fluxes between the land surface and atmospheric boundary layer at the small watershed-scale (~hundred meters in radius). However, this method has been primarily used in research to understand land use change impact on carbon and water fluxes (Brunsell et al., 2008; Fischer et al., 2012; Wagle and Kakani, 2014) because it is still cost-prohibitive for ET estimates at broad scales applicable to water resource management.

Remote sensing, using geostationary and polar-orbiting satellite imagery, is the most efficient approach for assessing ET over large spatial areas (Allen et al., 2011, 2007; Anderson et al., 2011; Mu et al., 2011). However, this approach is limited by time elapse between satellite images, making ET data using remote sensing typically available only a few days per week or month. For example, the Moderate Resolution Imaging Spectroradiometer (MODIS) sensor provides 8-day ET products generated with the algorithms of Mu et al. (2011). In addition, the coarse spatial resolutions (500–1000 m) of satellite imagery impede ET estimation and water resource management and research at the field or small watershed scale. Landsat imagery provides higher spatial resolution ET data (up to 30 m) utilizing algorithms such as Surface Energy Balance Algorithm for Land (SEBAL) and Mapping EvapoTranspiration at high Resolution and Internalized Calibration (METRIC) and has the potential to improve ET estimates for field-scale applications. But,

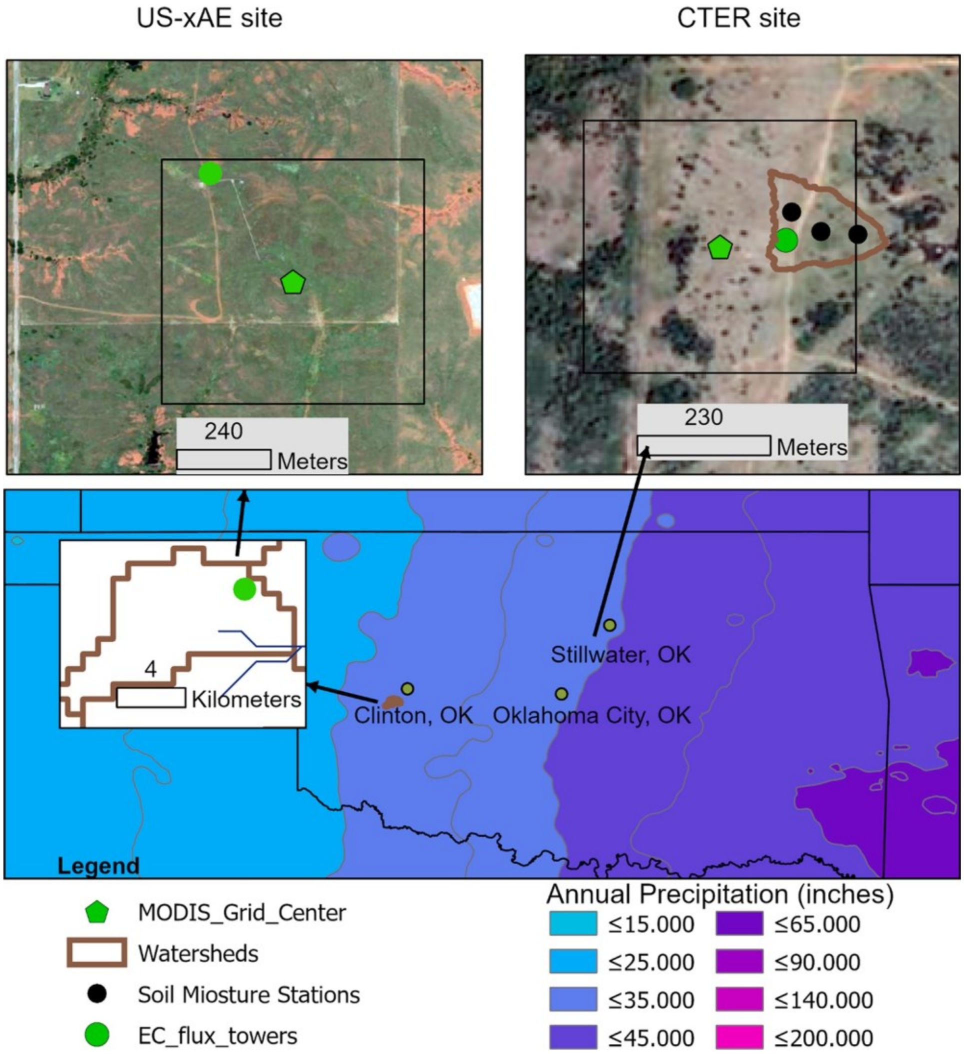

Fig. 1. The study sites of CTER and US-xAE with features of MODIS grid cells and EC flux towers. The annual precipitation was based on Parameter-elevation Regression on Independent Slopes Model (PRISM) 30-year normal precipitation climatology.

currently, Landsat ET products are mostly available and applicable for growing seasons of the irrigated crops (Allen et al., 2011).

The mechanistic framework of using biophysical models for simulating and scaling ET has proven effective for a range of scales from the field to the region. Bohn and Vivoni (2016) used the Variable Infiltration Capacity model, which produced the most realistic ET patterns for agricultural and forested mountain areas in the North American Monsoon region in comparison to several remote sensing-based products. Yang and Zhang (2016) applied the Soil and Water Assessment Tool (SWAT) to improve the ET and carbon assimilation simulations for North American forest ecosystems based on the AmeriFlux tower network. Alemayehu et al. (2017) modified SWAT to simulate vegetation growth in tropical ecosystems where rainfall, rather than temperature, is the dominant plant growth controlling factor. Utilizing intensively monitored experimental watersheds, Qiao et al. (2015) parameterized SWAT to simulate the distinct ecohydrological processes and vegetation impacts of native grasses and woody plants in the southern Great Plains (SGP). Although comparing ET estimates from remote sensing products has been carried out for different spatial-temporal scales worldwide (Abiodun et al., 2018; Dile et al., 2020; Khan et al., 2020; Odusanya et al., 2019), those using hydrological models for grassland-dominated ecosystems are relatively scarce at finer scales for upland areas of the southern Great Plains (SGP).

The SGP is a relatively water-limited region. Food production and environmental sustainability face increasing pressures from water shortage due to increasing climate variability and extensive human activities (e.g., extensive irrigation and Ogallala aquifer depletion). Much of the SGP has been transformed into different land use and land cover types and today is composed of a high percentage of croplands (e.g., wheat, cotton, and corn) and some urban areas (e.g., Dallas, TX, and Oklahoma City, OK). The physiographic setting includes higher and drier western high plains and lower and wetter central and eastern plains (Allred et al., 2015; Qiao et al., 2017 a and b; Engle et al., 2008).

Here, we mechanistically simulated ET for a tall-grass prairie and a mixed-grass prairie watershed using the biophysically-based SWAT model by incorporating soil moisture, energy balance, and available biomass production. Then, we used MODIS ET products to obtain separate ET estimates for the pixels representing the same tall-grass prairie and the mixed-grass prairie watersheds. Finally, we compared the SWAT and MODIS estimates to the baseline EC data and discussed the potential sources of errors from SWAT and MODIS and how climate and site-specific ecohydrological processes may have contributed to those errors. Our study is broadly applicable. The tall-grass and mixed-grass prairie biomes are the largest grassland ecosystems in the southern Great Plains, historically representing 246,560 km^2 out of 961,105 km^2 (Callan et al., 2016). Additionally, our study is relevant to analogous grassland systems that occur worldwide.

2. Study sites, data, and methods

2.1. Study sites and upland watershed description

The tall-grass prairie site was located at the Cross Timbers Experimental Range (CTER) near Stillwater, Oklahoma (36.0556° N, 97.1912°W), which is managed by the Oklahoma Agricultural Experiment Station (Fig. 1). This study site was initially cultivated in the 1930 s and reverted back to grassland when cultivation ceased (Zou et al., 2022). The vegetation is dominated by tall-grass prairie species composed of approximately 85% graminoid and 15% forb (Schmidt et al., 2021). Woody vegetation started to encroach into the grassland in the 1970 s and formed scattered woodland patches in some areas. Woody encroachment has been mostly controlled in the experimental watershed (Fig. 1). The main soil series in the watershed were the Stephenville-Darnell complex (64%) and the Coyle loam (20%). The slopes of the watershed range from 0% to 5%. The average soil depth is less than 1 m underlain by sandstone substrates (Zou et al., 2022).

The mixed-grass prairie was located at the NEON (National Ecological Observatory Network) Klemme Range Research Station (US-xAE) nearby Clinton, Oklahoma (35.4106° N, 99.0588° W) (Fig. 1). The most prominent grasses on the study site were buffalo grass (*Bouteloua dactyloides*) and purple three-awn (*Arisda purpurea*). The woody species included broom snakeweed (*Guerrezia sarothrae*) and small stature oaks as indicated by the Terrestrial Observation System (TOS), (2018). The watershed at this site has 1–5% slopes and its predominant soil series is Cordell silty clay loam eroded from the bedrock of shales (Soil Survey Geographic Database SSURGO (https://data.nal.usda.gov/dataset/soil-survey-geographic-database-ssurgo).

2.2. Meteorological variables and soil moisture data

The meteorological variables were collected daily for the two sites from the Oklahoma MESONET, an environmental monitoring network with approximately 120 stations across Oklahoma (McPherson et al., 2007). The nearest MESONET stations were 1.9 km and 1.1 km from the CTER and US-xAE sites, respectively. Meteorological data used in the study included precipitation, daily maximum temperature, daily minimum temperature, wind speed at 2 m above the ground, solar radiation, and relative humidity for the period of 1998 – 2021 (https://www.mesonet.org/index.php/weather/category/past_data_files). According to the data, the long-term mean annual precipitation for the CTER site was about 890 mm with average daily maximum and minimum temperatures of 22.3 °C and 9.3 °C, respectively. The long-term mean annual precipitation for the US-xAE site was about 770 mm, with average daily maximum and minimum temperatures of 23.1 °C and 9.3 °C, respectively.

Soil moisture measurements are very important for validating water balance simulations in SWAT. Soil moisture at the CTER site was directly measured with ECH_2O soil moisture sensors (Decagon, Pullman, WA, USA). Three soil moisture stations were distributed at the upper, middle, and bottom locations across the study watershed. Each station had four EC-5 sensors throughout the soil profile at depths of 5, 20, 45, and 80 cm, which were placed at the middle point of each of the four soil zones (0–10, 10–30, 30–60, and 60–100 cm) to calculate the total soil water storage (depth, mm) in the upper 1-meter soil profile (Zou et al., 2014). Soil moisture data for the US-xAE site were acquired from Ameriflux (http://ameriflux.lbl.gov/) associated with EC measurements (NEON, 2021). The data were measured at the upper and lower layers of the soil profile at the flux tower site. For both sites, soil water storage in the top 1 m was calculated.

2.3. Eddy covariance ET measurements

At the ecosystem scale, ET estimates from EC methods are considered the most accurate and, as such, were used as baseline ET estimates in this study. The EC system at CTER was installed in 2015 to collect carbon and water fluxes in the tall-grass prairie. These data were processed through a series of quality assurance/quality control measures and data gap filling methods published by Sun et al. (2019). The EC data for the US-xAE site (NEON, 2021) were available for 2017–2021 from the AmeriFlux network (http://ameriflux.lbl.gov/). However, we only selected the highest quality daily data from US-xAE site which had at least 18-hours of valid measurements, resulting in 204 daily points. We then grouped daily points into 8-day data starting from the first day of the year. Only groups with at least 4 valid daily points were used to calculate 8-day points (the average of the daily points). This resulted in 31 valid 8-day points during the period 2017–2021.

2.4. Remote sensing ET and net primary productivity

The updated remote sensing ET product MOD16A2 Version 6.1 (MOD16) (Running et al., 2017) was selected for our study. MOD16 provides an 8-day composite estimate of ET with a spatial resolution of 500 m. The MOD16 data were produced using the Penman-Monteith equation considering the daily meteorological data together with data for fraction of photosynthetically active radiation (FPAR), leaf area index (LAI), albedo, and land cover based on MODIS sensors onboard NASA's Terra/Aqua satellites (Mu et al., 2011).

Biomass data were also updated from the latest MOD17A2H version 6.1 (MOD17) Gross Primary Productivity (GPP) product which is also a cumulative 8-day composite of values with a 500 m spatial resolution (Running et al., 2015). This product is based on the radiation-use efficiency concept that shares information from several common bands used to calculate ET by MOD16 (Zhao et al., 2005; Zhao and Running, 2010). We converted the GPP to total net primary productivity (NPP) according to Zhao et al. (2005).

2.5. Biophysical SWAT model

The SWAT model is a biophysical and hydrological model with capacities to simulate water, carbon, and nutrient dynamics from areas ranging from small watersheds to larger river basins for agricultural management, land use and land cover change analysis, and climate change impact assessment (Abbaspour et al., 2015; Arnold and Allen, 1999; Arnold et al., 2012; Qiao et al., 2014, 2015; Zhang et al., 2007; Zou et al., 2015). The SWAT model in this study for the CTER site was initially configured and calibrated for runoff and soil water data for upland watersheds (2–5 ha) in the subhumid area of the SGP (Qiao et al., 2015). Since our SWAT model simulation was designed to estimate field-scale ecohydrological processes, fine resolution soil data from SSURGO and Light Detection and Ranging (LiDAR) (1.4 m) elevation data were obtained to define the hydrological response units (HRUs), river reaches, and watershed boundaries. The USGS National Land Cover Database (NLCD) was used to determine land cover classes in the model configuration using raster datasets having a spatial resolution of 30 m. This SWAT model was further tested for a broader region across the climate gradient zone of the SGP and had an acceptable performance for the semiarid and arid regions with even better performance than a similar model calibrated with streamflow measured at the river basin scales (Zou et al., 2015). The SWAT model for the US-xAE site was configured for this study using the same types of NLCD land use and SSURGO soil datasets mentioned above. However, the basins

Table 1
Parameters' ranges and optimal values identified with the SPUCI global optimization algorithm.

Parameter Names	Parameter Values		
	Lower bound	Upper bound	Optimal Values for CTER and US-xAE Sites
r_CN2 (Curve Number)	-0.2	0.2	-0.072
v_ESCO (soil evaporation compensation factor)	0.5	1	0.911
v_GW_REVAP (ground water revap coefficient)	0.02	0.1	0.078
v_CANMX (maximum canopy interception, mm)	0.27	3	0.743
r_SOL_AWC (soil available water content, mm)	0.1	0.3	0.211
r_SOL_K (soil saturation hydraulic conductivity, mm/hr)	-0.6	-0.1	-0.344
r_SOL_BD (soil bulk density, g/cc)	-0.3	-0.1	-0.225
v_T_OPT (plant optimal growth temperature,°C)	18	24	21.077
v_T_BASE (plant base growth temperature,°C)	8	13	10.445
v_BIO_E (energy use efficiency)	30	50	33.270
v_BLAI (maximum leaf area index)	2	4	2.859
v_GSI (maximum stomatal conductance, m/s)	0.001	0.01	0.004

r: relative change of parameter values compared to their defaults based on SSURGO. For example, if original value is 100, + 2% change means 100 + 100 * 2% = 102.
v: absolute change of parameter values in their ranges

and HRUs were defined by USGS 30 m Digital Elevation Model (DEM) since we initially targeted a broad semiarid grassland in the SGP. The site locations and watershed boundaries along with their climate and land cover were shown in Fig. 1.

Leveraging the SWAT model's existing capacities for assessing runoff and soil water dynamics, we further improved the ET, biomass, and carbon component simulations by adjusting the parameters of maximum canopy storage (CANMX), LAI, and stomatal conductance (GSI), in addition to runoff and soil water controlling parameters. We used the Penman-Monteith equation to calculate potential evapotranspiration (PET). Actual ET was then partitioned into plant canopy evaporation, plant transpiration, and soil evaporation. The other series of important parameters such as radiation use efficiency (Bio_E), optimal temperature (T_OPT), and base temperature (T_BASE) for plant growth were calibrated for optimal grass growth and carbon assimilation. These are also sensitive parameters for plant growth, biomass production, and water use in biofuel crops and trees (Trybula et al., 2015; Guo et al., 2019).

Both SWAT models for CTER and US-xAE sites were run for 1998–2016 with MESONET meteorological data. The period 1998–2005 was used as a warming-up period to sufficiently minimize the effects of initial state variables on model outputs. The model outputs from 2016 to 2021 were used as the final dataset to compare with on-site ET measurement. EC data at the CTER site was only available for 2016, so the entire dataset was used for model calibration. Validation was carried out with the data available at the US-xAE site. There were 5 years of EC data (2017–2021) for the US-xAE site but with a significant number of low-quality data points. That means we only selected the daily data point with measurements for more than 18 h each day, as described in Section 2.3. Table 1 shows the parameter ranges and optimal parameter values identified with the SPUCI (shuffled complex evolution with principal component analysis) algorithm (Chu et al., 2010), a global parameter optimization method for high dimensional and complex problems.

2.6. Evaluation metrics

R^2 (squared Pearson correlation coefficient) and percent bias were used to identify the ET prediction accuracies from SWAT and MODIS compared to flux tower measurements. R^2 can help us see the dynamic correlation (if the two variables are closely scattered to the 1:1 ratio line) while percent bias can tell how much overestimates/underestimates are there.

3. Results

3.1. Aridity index for the two sites

For the period 2016–2021, annual precipitation was consistently higher at the subhumid CTER site (740–1370 mm) than at the semiarid US-xAE site (660–950 mm) (Fig. 2A). The minimum precipitation occurred in 2021 for both sites and the maximum precipitation occurred in 2019, which was an exceptionally wet year (480 mm higher than long-term annual average at the CTER site). Potential evapotranspiration (PET) was consistently lower at the subhumid CTER site (1170–1370 mm) than at the semiarid US-xAE site (1500–1650 mm) during the analysis period (Fig. 2B). As a result, the aridity index (AI), the ratio of annual precipitation to annual PET, was consistently higher at the CTER (0.6–1.2) than at the US-xAE (0.3–0.6). The AI value of 0.45 separates subhumid (above 0.45) and semiarid (below 0.45) climate zones. During the study period, the CTER site was always in the subhumid condition, while US-xAE was in the semi-arid condition for four of the six years.

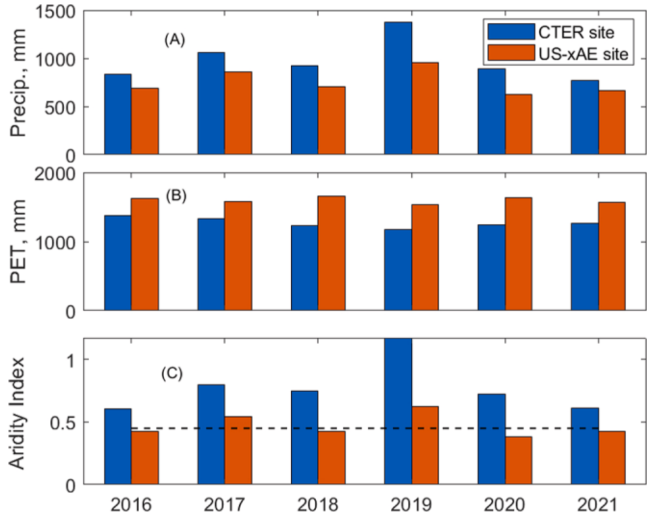

Fig. 2. Annual precipitation (A), potential evapotranspiration (B), and aridity index (C) for the CTER and US-xAE sites. The dark dash line represents the value 0.45, which separates subhumid (above) and semiarid (below) climate zones.

3.2. ET estimates from three different sources

All of the three different ET sources - EC flux tower (ET_Tower), SWAT simulation (ET_SWAT), and MODIS remote sensing products (ET_MOD16) - measured or simulated higher actual evapotranspiration (ET) at the CTER site than at the US-xAE site during 2016–2021 (Fig. 3). ET_Tower and ET_SWAT were originally available at half-hour and daily scales, respectively, but the comparison was made at the 8-day temporal scale since the ET_MOD16 was only available at that temporal resolution. The maximum ET each year was above 30 mm/8-day at the CTER site, while it was mostly below 30 mm/8-day at the US-xAE site from all three sources. Compared to the available ET_Tower data, there were relatively small biases (−0.40% and 5.04%) for the CTER site from ET_SWAT and ET_MOD16, respectively, for 2016. However, the ET_SWAT had much less bias than the ET_MOD16 for the US-xAE site with − 1.78% versus − 45.71% during 2016–2021. The MODIS ET product tended to overestimate ET for the subhumid area and underestimate ET for the semiarid area throughout the study period, especially for the peak water use seasons, regardless of the relative wetness or dryness of the year. One-way ANOVA tests showed $p = 0.924$ and 0.0004 for the CTER and the US-xAE site, respectively, suggesting that the three ET sources were not significantly different for the CTER site but significantly different for the US-xAE site. Table 2 showed the specific p values following the ANOVA test for each pair of the three ET sources, which showed no significant difference between ET-Tower and ET-SWAT ($p = 0.9954$). At the same time, there was a significant difference between ET-Tower and ET-MOD16 ($p = 0.0015$).

The scatter plots and regression lines between ET_TOWER and the two sources of ET_SWAT and ET_MOD16 also showed promising ET simulations for the CTER site with comparable R^2 values (0.77 and 0.87), but a much better performance of ET_SWAT than ET_MOD16 with R^2 values of 0.68 and 0.13 for the US-xAE site (Fig. 4). All regression lines in the figure are statistically significant ($p < 0.05$) using F-statistic test.

3.3. Soil moisture comparison between SWAT and in-situ observations

The daily soil water storage anomalies during 2016–2021 for the CTER and US-xAE sites were shown in Fig. 5 for both field observations and SWAT simulations. Anomalies were identified when the daily soil moisture deviated from the multiple-year average. Exceptionally dry soils usually appeared during the summer season from June to August at both sites. In addition, the semiarid US-xAE region also experienced prolonged dry soil conditions in 2020 and 2021 which were not prominent in the subhumid prairies of the CTER site. The SWAT model captured the soil water dynamics better for the CTER site with R^2 of 0.50 for 2016, compared to the US-xAE site with R^2 of 0.30 for the years 2019–2020. This could be partly ascribed to better soil moisture representation at the CTER site than at the US-xAE site, as more stations (3 vs.1) were measured at the former than at the latter site.

3.4. NPP estimates from SWAT and MODIS products

NPP estimates during peak growth periods were lower from the SWAT simulation than from the remote sensing estimation (MOD17) for the CTER site, while they were generally higher in SWAT simulation than the MOD17 estimation for the US-xAE site (Fig. 6). For both sites, MOD17 had much greater NPP estimates than SWAT during the dormant period of late fall to early spring, driving the total annual NPP from MOD17 to be substantially higher. Conversely, SWAT exhibited a significant number of dormant days without any NPP. Overall, only weak correlations were observed between SWAT and MOD17 NPP estimates during the peak growth periods, with R^2 values of 0.46 for both the CTER and US-xAE sites.

4. Discussion

Most ET estimations for the SGP focus on remote sensing approaches using statistical models linking vegetation indices with plant

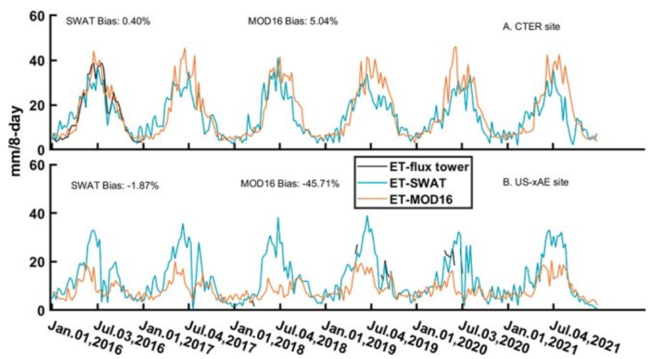

Fig. 3. ET (8-day) time series (2016–2021) of EC tower measurements, SWAT simulation, and MOD16 for CTER (A) and US-xAE (B) in Oklahoma, USA. The bias values are calculated for CTER and US-xAE using the data shown in black lines, respectively, limited by the dataset availability. One-way ANOVA tests showed $p = 0.924$ and 0.0004 for CTER and US-xAE sites, respectively, suggesting that the three ET sources are not significantly different for the CTER site but significantly different for the US-xAE site.

Table 2
One-way ANOVA test for the three ET estimates (ET-flux tower, ET-SWAT, and ET-MOD16) of the US-xAE site.

Group A	Group B	Lower Limit	A-B	Upper Limit	P-value
ET-flux tower	ET-SWAT	-4.4545	0.1772	4.8090	0.9954
ET-flux tower	ET-MOD16	2.3443	6.9760	11.6080	0.0015
ET-SWAT	ET-MOD16	2.1670	6.7988	11.4300	0.0021
ET-SWAT	ET-MOD16	2.1670	6.7988	11.4300	0.0021

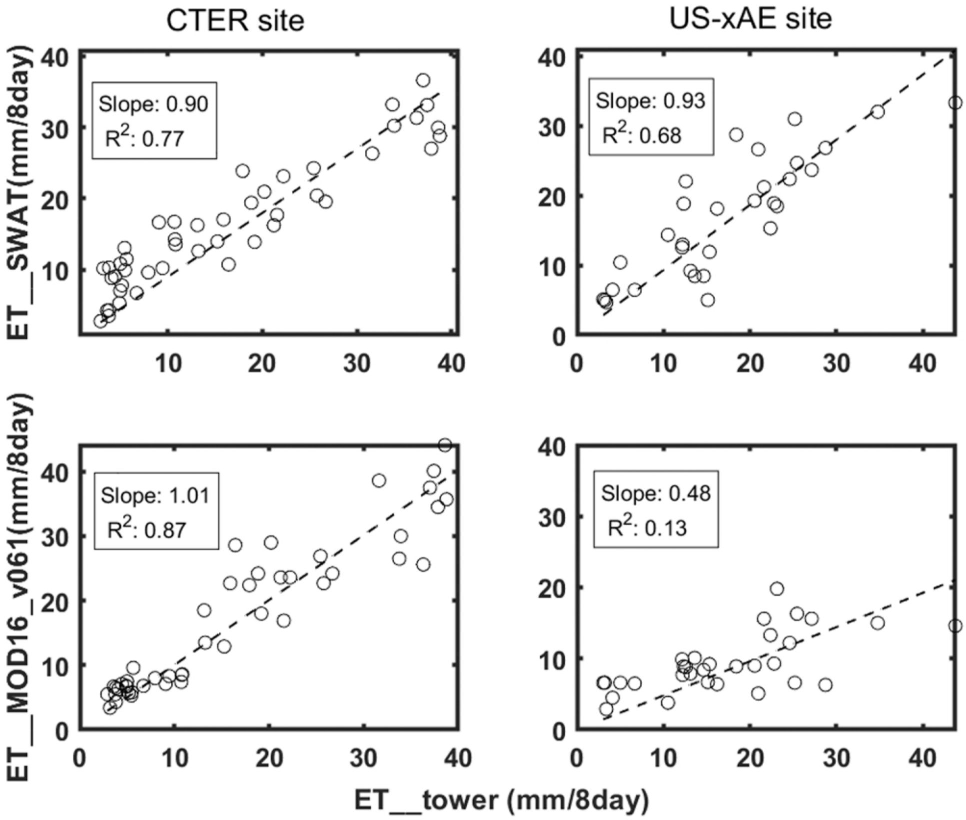

Fig. 4. Linear regressions of 8-day ET simulations of SWAT (upper) and MOD16 (lower) against EC flux measurements for CTER (left column) and US-xAE (right column) in Oklahoma, USA. All regression lines are statistically significant ($p < 0.05$) using the F-statistic test.

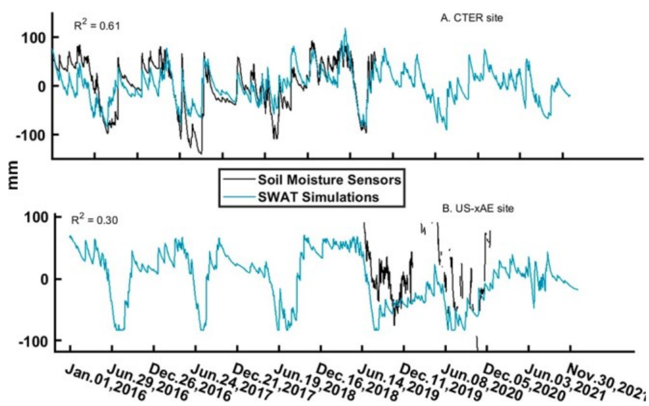

Fig. 5. Soil water storage anomalies of field observations and SWAT simulations for CTER (A) and US-xAE (B) in Oklahoma, USA.

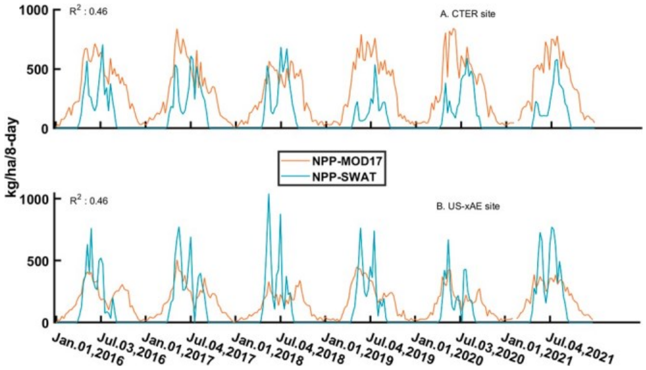

Fig. 6. Net primary productivity (NPP) (8-day) time series (2016–2021) from SWAT simulation and MOD17 for CTER (A) and US-xAE (B) sites in Oklahoma, USA. R^2 values of the linear relation between SWAT simulation and MOD17 were calculated only for growing seasons.

growth and water use (e.g., Wagle and Kakani, 2014). MODIS products in this study provided slight ET overestimation (~ 5%) for the subhumid site but with considerable underestimation (over 40%) for the semiarid site, suggesting that the vegetation indices-based approach has limitations in this region. Many studies have indicated that misclassification of land cover and land use greatly contributes to errors in MOD16 algorithms (Ruhoff et al., 2013). This could be the case for both the semiarid and subhumid grasslands in the SGP, where grasses, shrubs, and trees frequently coexist within a small area (i.e., less than the pixel size of 500 m), which could cause misrepresentation of the fraction of photosynthetically active radiation (FPAR), leaf area index, leaf phenology, and albedo for the grasslands (Fig. 1). MODIS estimates of ET and NPP are based on these biophysical parameters, making classification variability a primary source of error.

In this study, SWAT better reflected the biophysical mechanisms driving ET for the SGP grasslands, outperforming the MODIS products in various aspects of water and productivity dynamics. ET flux measured with EC towers usually has ± 10% bias (Moorhead et al., 2019), and the SWAT model's bias is within/close to this range. The SWAT model also performed well in simulating the soil water storage dynamics for the tall-grass prairie (subhumid region). The soil water storage anomalies of field observations and SWAT simulations for the mixed-grass prairie (semiarid region) were much greater than for the tall-grass prairie (Fig. 5). A possible reason is that only one soil moisture field observation was available and used for comparison for the mixed-grass prairie. While no empirical intra-annual estimates of NPP were available, annual calculations of NPP based on clip plots were much closer to SWAT-based than MOD17-based annual estimates for the subhumid grassland sites. Fig. 7 compares the SWAT-based NPP estimates from the subhumid site from 2014 to 2016 with direct measurements of NPP based on aboveground NPP (ANPP) using clip plots (Schmidt et al., 2021). Because the clip plot was only for aboveground production, we converted these to total NPP by assuming that ANPP is 46% of the total (Xu et al., 2012). After doing so, the SWAT-based estimates of NPP were much closer to estimates from clip plots, while the MODIS products overestimated NPP by almost 100%.

There were robust linear correlations between the MODIS estimates of ET and NPP (Fig. 8a), with R^2 mostly greater than 0.60 each year for both sites. Compared to the SWAT estimates, NPP peaks were slightly overestimated by the MODIS product of MOD17 (Fig. 6A), which corresponded to a slightly higher ET estimation of MOD16 (Fig. 3A) for the subhumid site. The peaks of NPP were considerably underestimated when estimated by MOD17 for the semiarid site (Fig. 6B), which corresponded to a much lower ET estimation in the product (Fig. 3B).

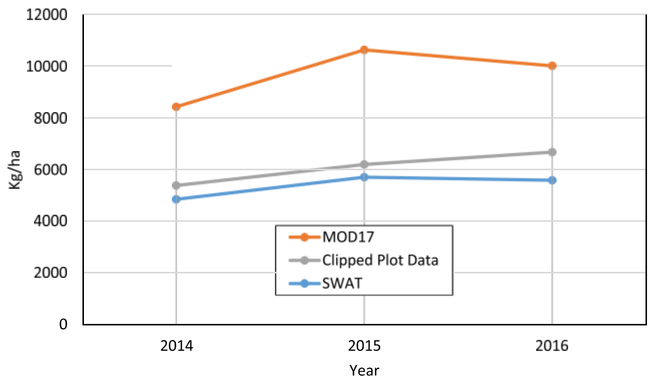

Fig. 7. Annual NPP at the subhumid CTER site from 2014 to 2016 from SWAT simulation, MOD17 (NPP), field measurement of clip plot data (aboveground NPP). Estimates from clip plots were collected as aboveground NPP and converted to total NPP, assuming that aboveground NPP is 46% of the total (Xu et al., 2012).

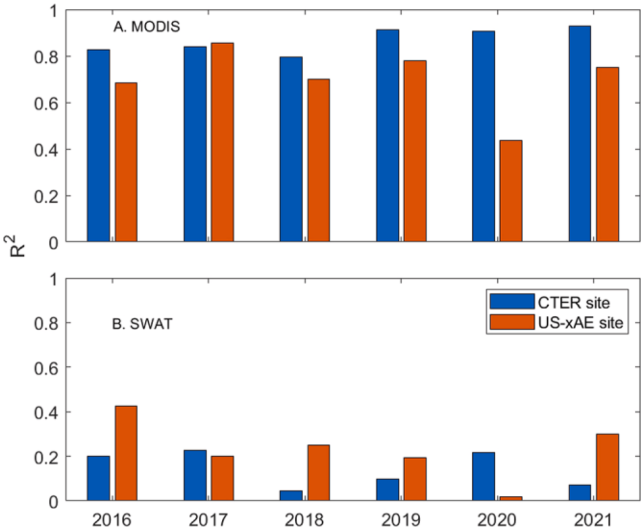

Fig. 8. The R^2 of linear correlations between 8-day NPP and ET in the remote sensing data of MODIS (A) and SWAT simulations (B) for CTER and US-xAE sites.

In SWAT simulations, ET and NPP were weakly correlated with R^2 mostly lower than 0.30 for each year from 2016 to 2021 (Fig. 8b). At the CTER site, the ratio of transpiration and ET (T/ET) ranged from 0.84 to 0.92 during the 2016 growing season (Sun et al., 2021). We did not have T/ET data for the US-xAE site, but Scott et al. (2005) reported a ratio of 0.84 for the growing season in the semiarid grasslands of Arizona and Moran et al. (2009) reported a ratio of 0.76 based on a different estimation approach using diurnal soil temperature measurements for a longer time period (2004–2006). The high T/ET ratios should result in a strong correlation between ET and NPP, at least during the growing season for both sites. It remains unknown why the correlation between ET and NPP from SWAT simulation was so weak (Fig. 8b). One explanation would be that the SWAT model parameterization did not represent the right proportion of evaporation and transpiration even though the total ET quantity was correctly simulated. Models with a large number of parameters tend to experience non-uniqueness problems that models can be fit equally well by a multitude of parameter vectors (Abbaspour et al., 2007; Leta et al., 2015). Here we targeted the total ET quantity and did not explicitly consider transpiration and evaporation separately so that compensation could happen between them. SWAT uses soil water compensation factor, plant uptake compensation factor, root density and depth, and other biophysical parameters (as mentioned in Table 1) in addition to soil water dynamics and atmospheric conditions. Due to model structure and parameter uncertainty, it is still challenging to properly partition ET into transpiration and evaporation in SWAT and other ecohydrological models. Another explanation would be that transpiration may not dominate the total ET for SGP grasslands. Some studies found that evaporation may account for a greater percentage of ET in many semiarid-subhumid settings (Huxman et al., 2005; Kurc et al., 2004). The reasoning is that direct evaporation is only contributed by the top 20 cm of soil which accumulates most rainfall inputs in dry climates (Boulet et al., 1997; Yamanaka and Yonetani, 1999). More efforts are needed to clarify this issue in future studies.

Soil moisture is the primary limiting factor driving ecohydrological processes in water-limited systems. The overall better performance of the SWAT model may be attributed to its inclusion of soil moisture information in the simulation, while MODIS algorithms do not include soil moisture information. More consistent and better representation of soil moisture conditions for the subhumid region may explain why ET was better simulated for the subhumid region than for the semiarid region by the hydrological model and MODIS remote sensing products in this study. The CTER site is located in the ecosystem transition zone with very high annual climate variabilities. However, the rainfall regime in the semiarid region is characterized by even greater spatial and temporal variabilities. The more sporadic and infrequent rainfall in the drier grasslands and the vertical distribution of soil moisture along the rooting zone is usually quite variable, and the soil water storage term is subject to greater errors (Fig. 5), which will increase the uncertainty and errors of estimates of ET and NPP from both hydrological models and remote sensing products.

The mechanistic framework of using biophysical models simulating ET has been proven effective from the field to regional scales (Bohn and Vivoni, 2016; Yang and Zhang, 2016). Remote sensing ET of MODIS requires relatively less input information to cover a rather large spatial scale. Due to its availability, many hydrological models have used remote sensing ET as their calibration inputs for model improvement (Amatya et al., 2016; Immerzeel and Droogers, 2008; Parajuli et al., 2018; Rajib et al., 2016; Tobin and Bennett, 2017; Zhang et al., 2017). This study suggests that a more thorough evaluation of the remote sensing ET product would be beneficial before its application since it could provide different accuracies for different climate and vegetation conditions.

5. Conclusions

Hydrological models and remote sensing are two common tools to estimate evapotranspiration at the ecosystem scale. Both SWAT simulation and MODIS products produced relatively accurate ET estimates in the subhumid tall-grass prairie of the southern Great

Plains (SGP). In contrast, the SWAT simulation performed better than the MODIS products for the semiarid, mixed-grass prairie, where the MODIS products considerably underestimated ET (over 40%). Mechanistically simulated ET utilizing the biophysical SWAT model shows higher potential to approximate the evapotranspiration and biomass growth processes than the MODIS remote sensing approaches in both subhumid and semiarid grasslands of the SGP. However, it is still not validated for partitioning evaporation and transpiration in the SWAT model due to parameter uncertainties caused by complicated water flows in the soil-plant continuum in the SWAT (Though E is domonating suggested by the model for the grass praries). This study provides a more accurate ET estimation approach. It adds new insights into the upscaling of spatially distributed ET, soil water, plant biomass, and thus water resources management in tall-grass prairie and mixed grass prairies of the southern Great Plains of the USA.

CRediT authorship contribution statement

Lei Qiao: Conceptualization, Methodology. **Chris Zou:** Conceptualization, Methodology. **Rodney Will:** Conceptualization, Methodology. **Lei Qiao:** Data curation, Writing – original draft. **Lei Qiao:** Visualization, Investigation. **Rodney Will:** Visualization, Investigation. **Chris Zou:** Visualization, Investigation. **Kevin Wagner:** Visualization, Investigation. **Tian Zhang:** Visualization, Investigation. **Rodney Will:** Writing – review & editing. **Chris Zou:** Writing – review & editing. **Kevin Wagner:** Writing – review & editing. **Tian Zhang:** Writing – review & editing.

Declaration of Competing Interest

The authors declare that they have no known competing financial interests or personal relationships that could have appeared to influence the work reported in this paper.

Data Availability

Data will be made available on request.

Acknowledgments

This research was partly supported by the USDA-ARS Dam Analysis Modernization of Tools, Applications, Guidance and Standardization (DAM-TAGS) Project (3072-13000-010-048-S) and USDA-NIFA McIntire Stennis OKL03151 and OKL03152, and the National Science Foundation under Grant No. OIA-1946093, and the endowment for the Sarkeys Distinguished Professorship.

References

Abbaspour, K.C., Yang, J., Maximov, I., Siber, R., Bogner, K., Mieleitner, J., Zobrist, J., Srinivasan, R., 2007. Modelling hydrology and water quality in the pre-alpine/alpine Thur watershed using SWAT. J. Hydrol. 333 (2–4), 413–430.

Abbaspour, K.C., Rouholahnejad, E., Vaghefi, S., Srinivasan, R., Yang, H., Kløve, B., 2015. A continental-scale hydrology and water quality model for Europe: calibration and uncertainty of a high-resolution large-scale SWAT model. J. Hydrol. 524 (0), 733–752.

Abiodun, O.O., Guan, H., Post, V.E.A., Batelaan, O., 2018. Comparison of MODIS and SWAT evapotranspiration over a complex terrain at different spatial scales. Hydrol. Earth Syst. Sci. 22 (5), 2775–2794.

Alemayehu, T., van Griensven, A., Woldegiorgis, B.T., Bauwens, W., 2017. An improved SWAT vegetation growth module and its evaluation for four tropical ecosystems. Hydrol. Earth Syst. Sci. 21 (9), 4449–4467.

Alfieri, J.G., Blanken, P.D., Smith, D., Morgan, J., 2009. Concerning the measurement and magnitude of heat, water vapor, and carbon dioxide exchange from a Semiarid Grassland. J. Appl. Meteorol. Climatol. 48 (5), 982–996.

Allen, R., Irmak, A., Trezza, R., Hendrickx, J.M.H., Bastiaanssen, W., Kjaersgaard, J., 2011. Satellite - based ET estimation in agriculture using SEBAL and METRIC. Hydrol. Process. 25 (26), 4011–4027.

Allen, R.G., Tasumi, M., Morse, A., Trezza, R., Wright, J.L., Bastiaanssen, W., Kramber, W., Lorite, I., Robison, C.W., 2007. Satellite-based energy balance for mapping evapotranspiration with internalized calibration (METRIC) - applications. J. Irrig. Drain. Eng. 133 (4), 395–406.

Allred, B.W., Smith, W.K., Twidwell, D., Haggerty, J.H., Running, S.W., Naugle, D.E., Fuhlendorf, S.D., 2015. Ecosystem services lost to oil and gas in North America. Science 348 (6233), 401–402.

Amatya, D.M., Irmak, S., Gowda, P., Sun, G., Nettles, J.E., Douglas-Mankin, K.R., 2016. Ecosystem evapotranspiration: challenges in measurements, estimates, and modeling. Trans. ASABE 59, 555–560.

Anderson, M.C., Kustas, W.P., Norman, J.M., Hain, C.R., Mecikalski, J.R., Schultz, L., Gonz´alez-Dugo, M.P., Cammalleri, C., d'Urso, G., Pimstein, A., Gao, F., 2011. Mapping daily evapotranspiration at field to continental scales using geostationary and polar orbiting satellite imagery. Hydrol. Earth Syst. Sci. 15 (1), 223–239.

Terrestrial Observation System (TOS), 2018. Site Characterization Report: Domain 11. NEON.DOC.003894vB

AnonNEON (National Ecological Observatory Network),. 2021. AmeriFlux BASE US-xAE NEON Klemme Range Research Station (OAES), Ver. 3–5, AmeriFlux AMP, (Dataset). 〈https://doi.org/10.17190/AMF/1671891〉.

Arnold, J.G., Allen, P.M., 1999. Automated methods for estimatiating baseflow and ground water recharge from streamflow records. JAWRA J. Am. Water Resour. Assoc. 35 (2), 411–424.

Arnold, J.G., Moriasi, D.N., Gassman, P.W., Abbaspour, K.C., White, M.J., Srinivasan, R., Santhi, C., Harmel, R.D., Van Griensven, A., Van Liew, M.W., Kannan, N., Jha, M.K., 2012. SWAT: Model use, calibration, and validation. Trans. ASABE 55 (4), 1491–1508.

Bohn, T.J., Vivoni, E.R., 2016. Process-based characterization of evapotranspiration sources over the North American monsoon region. Water Resour. Res. 52 (1), 358–384.

Boulet, G., Braud, I., Vauclin, M., 1997. Study of the mechanisms of evaporation under arid conditions using a detailed model of the soil–atmosphere continuum. Application to the EFEDA I experiment. J. Hydrol. 193 (1), 114–141.

Brunsell, N.A., Ham, J.M., Owensby, C.E., 2008. Assessing the multi-resolution information content of remotely sensed variables and elevation for evapotranspiration in a tall-grass prairie environment. Remote Sens. Environ. 112 (6), 2977–2987.

Callan, R., Leinwand, I.I.F., Reese, G.C., Assal, T.J., Manier, D.J., Carr, N.B., Burris, Lucy, Ignizio, D.A., 2016. Estimated historical distribution of grassland communities of the Southern Great Plains: U.S. Geological Survey data release, 〈https://dx.doi.org/10.5066/F71Z42J3〉.

Chu, W., Gao, X., Sorooshian, S., 2010. Improving the shuffled complex evolution scheme for optimization of complex nonlinear hydrological systems:application to the calibration of the sacramento soil-moisture accounting model. Water Resour. Res. 46 (9).

Diego, G.M., Raquel, N., Nathan, G.M., Wouter, A.D., Niko, E.C.V., Yi, Y.L., Adriaan, J.T., Dolman, A.J., Stephen, P.G., Luis, G., 2016. Contribution of water-limited ecoregions to their own supply of rainfall. Environ. Res. Lett. 11 (12), 124007.

Dile, Y.T., Ayana, E.K., Worqlul, A.W., Xie, H., Srinivasan, R., Lefore, N., You, L., Clarke, N., 2020. Evaluating satellite-based evapotranspiration estimates for hydrological applications in data-scarce regions: A case in Ethiopia. Sci. Total Environ. 743, 140702.

Engle, D., Coppedge, B., Fuhlendorf, S., 2008. From the Dust Bowl to the Green Glacier: Human Activity and Environmental Change in Great Plains Grasslands. In: Auken, O.W. (Ed.), Western North American Juniperus Communities. Ecological Studies. Springer, New York, pp. 253–271.

Fischer, M.L., Torn, M.S., Billesbach, D.P., Doyle, G., Northup, B., Biraud, S.C., 2012. Carbon, water, and heat flux responses to experimental burning and drought in a tall-grass prairie. Agric. For. Meteorol. 166, 169–174.

Guo, T., Engel, B.A., Shao, G., Arnold, J.G., Srinivasan, R., Kiniry, J.R., 2019. Development and improvement of the simulation of woody bioenergy crops in the Soil and Water Assessment Tool (SWAT). Environ. Model. Softw. 122, 104295.

Huxman, T.E., Wilcox, B.P., Breshears, D.D., Scott, R.L., Snyder, K.A., Small, E.E., Hultine, K., Pockman, W.T., Jackson, R.B., 2005. Ecohydrological implications of woody plant encroachment. Ecology 86 (2), 308–319. https://doi.org/10.1890/03-0583.

Immerzeel, W.W., Droogers, P., 2008. Calibration of a distributed hydrological model based on satellite evapotranspiration. J. Hydrol. 349, 411–424.

Johnson, D.A., Nicanor, Z.S., John, W.W., Hendrickson, J.R., 2003. Bowen ratio versus canopy chamber CO_2 fluxes on sagebrush rangeland. J. Range Manag. 56 (5), 517–523.

Khan, M.S., Baik, J., Choi, M., 2020. Inter-comparison of evapotranspiration datasets over heterogeneous landscapes across Australia. Adv. Space Res. 66 (3), 533–545.

Kurc, S.A., Small, E.E., 2004. Dynamics of evapotranspiration in semiarid grassland and shrubland ecosystems during the summer monsoon season, central New Mexico. Water Resour. Res. 40 (9) https://doi.org/10.1029/2004WR003068.

Kurc, S.A., Small, E.E., 2007. Soil moisture variations and ecosystem - scale fluxes of water and carbon in semiarid grassland and shrubland. Water Resour. Res. 43 (6).

Leta, O.T., Nossent, J., Velez, C., Shrestha, N.K., Van Griensven, A., Bauwens, W., 2015. Assessment of the different sources of uncertainty in a SWAT model of the River Senne (Belgium). Environ. Model. Softw. 68, 129–146.

Lu, N., Chen, S., Wilske, B., Sun, G., Chen, J., 2011. Evapotranspiration and soil water relationships in a range of disturbed and undisturbed ecosystems in the semi-arid Inner Mongolia, China. J. Plant Ecol. 4 (1–2), 49–60.

McPherson, R.A., Fiebrich, C.A., Crawford, K.C., Kilby, J.R., Grimsley, D.L., Martinez, J.E., Basara, J.B., Illston, B.G., Morris, D.A., Kloesel, K.A., Melvin, A.D., Shrivastava, H., Wolfinbarger, J.M., Bostic, J.P., Demko, D.B., Elliott, R.L., Stadler, S.J., Carlson, J.D., Sutherland, A.J., 2007. Statewide Monitoring of the Mesoscale Environment: A Technical Update on the Oklahoma Mesonet. J. Atmos. Ocean. Technol. 24 (3), 301–321.

Moorhead, J.E., Marek, G.W., Gowda, P.H., Lin, X., Colaizzi, P.D., Evett, S.R., Kutikoff, S., 2019. Evaluation of evapotranspiration from Eddy covariance using large weighing lysimeters. Agronomy 9 (2), 99. https://doi.org/10.3390/agronomy9020099.

Moran, M.S., Scott, R.L., Keefer, T.O., Emmerich, W.E., Hernandez, M., Nearing, G.S., Paige, G.B., Cosh, M.H., O'Neill, P.E., 2009. Partitioning evapotranspiration in semiarid grassland and shrubland ecosystems using time series of soil surface temperature. Agric. For. Meteorol. 149 (1), 59–72.

Mu, Q., Zhao, M., Running, S.W., 2011. Improvements to a MODIS global terrestrial evapotranspiration algorithm. Remote Sens. Environ. 115 (8), 1781–1800.

Norris, M.D., Blair, J.M., Johnson, L.C., McKane, R.B., 2001. Assessing changes in biomass, productivity, and C and N stores following Juniperus virginiana forest expansion into tall-grass prairie. Can. J. . Res. -Rev. Can. Rech. 31 (11), 1940–1946.

Odusanya, A.E., Mehdi, B., Schürz, C., Oke, A.O., Awokola, O.S., Awomeso, J.A., Adejuwon, J.O., Schulz, K., 2019. Multi-site calibration and validation of SWAT with satellite-based evapotranspiration in a data-sparse catchment in southwestern Nigeria. Hydrol. Earth Syst. Sci. 23 (2), 1113–1144.

Parajuli, P.B., Jayakody, P., Ouyang, Y., 2018. Evaluation of using remote sensing evapotranspiration data in SWAT. Water Resour. Manag. 32, 985–996.

Qiao, L., Pan, Z., Herrmann, R.B., Hong, Y., 2014. Hydrological variability and uncertainty of lower Missouri River Basin under changing climate. JAWRA J. Am. Water Resour. Assoc. 50 (1), 246–260.

Qiao, L., Zou, C.B., Will, R.E., Stebler, E., 2015. Calibration of SWAT model for woody plant encroachment using paired experimental watershed data. J. Hydrol. 523 (0), 231–239.

Qiao, L., Zou, C.B., Gait´an, C.F., Hong, Y., McPherson, R.A., 2017a. Analysis of precipitation projections over the climate gradient of the Arkansas-Red River Basin. J. Appl. Meteorol. Climatol. 56 (5), 1325–1336.

Qiao, L., Zou, C.B., Stebler, E., Will, R.E., 2017b. Woody plant encroachment reduces annual runoff and shifts runoff mechanisms in the tall-grass prairie, USA. Water Resour. Res. 53 (6), 4838–4849.

Rajib, M.A., Merwade, V., Yu, Z.Q., 2016. Multi-objective calibration of a hydrologic model using spatially distributed remotely sensed/in-situ soil moisture. Journal of Hydrology 536, 192–207.

Ruhoff, A.L., Paz, A.R., Aragao, L.E.O.C., Mu, Q., Malhi, Y., Collischonn, W., Rocha, H.R., Running, S.W., 2013. Assessment of the MODIS global evapotranspiration algorithm using eddy covariance measurements and hydrological modelling in the Rio Grande basin. Hydrol. Sci. J. 58 (8), 1658–1676.

Running, S., Mu, Q., Zhao, M., MOD17A2H MODIS/Terra Gross Primary Productivity 8-Day L4 Global 500m SIN Grid V006. 2015, distributed by NASA EOSDIS Land Processes DAAC, 〈https://doi.org/10.5067/MODIS/MOD17A2H.006〉.

Running, S., Mu, Q., Zhao, M., MOD16A2 MODIS/Terra Net Evapotranspiration 8-Day L4 Global 500m SIN Grid V006. 2017, distributed by NASA EOSDIS Land Processes DAAC, 〈https://doi.org/10.5067/MODIS/MOD16A2.006〉.

Schmidt, K.N., Zou, C.B., Kakani, V.G., Zhong, Y., Will, R.E., 2021. Improved productivity, water yield, and water use efficiency by incorporating switchgrass cultivation and native ecosystems in an integrated biofuel feedstock system. GCB Bioenergy 13, 369–381. https://doi.org/10.1111/gcbb.12787.

Scott, R.L., Huxman, T.E., Cable, W.L., Emmerich, W.E., 2006a. Partitioning of evapotranspiration and its relation to carbon dioxide exchange in a Chihuahuan Desert shrubland. Hydrol. Process. 20 (15), 3227–3243.

Scott, R.L., Huxman, T.E., Cable, W.L., Emmerich, W.E., 2006b. Partitioning of evapotranspiration and its relation to carbon dioxide exchange in a Chihuahuan Desert shrubland. Hydrol. Process. 20 (15), 3227–3243.

Sun, X., Zou, C.B., Wilcox, B., Stebler, E., 2019. Effect of vegetation on the energy balance and evapotranspiration in Tall-grass Prairie: a paired study using the Eddy-Covariance method. Bound. -Layer. Meteor. 170, 127–160. https://doi.org/10.1007/s10546-018-0388-9.

Tobin, K.J., Bennett, M.E., 2017. Constraining swat calibration with remotely sensed evapotranspiration data. J. Am. Water Resour. Assoc. 53, 593–604.

Todd, R.W., Evett, S.R., Howell, T.A., 2000. The Bowen ratio-energy balance method for estimating latent heat flux of irrigated alfalfa evaluated in a semi-arid, advective environment. Agric. For. Meteorol. 103 (4), 335–348.

Trybula, E.M., Cibin, R., Burks, J.L., Chaubey, I., Brouder, S.M., Volenec, J.J., 2015. Perennial rhizomatous grasses as bioenergy feedstock in SWAT: parameter development and model improvement. GCB Bioenergy 7 (6), 1185–1202.

Van Auken, O.W., 2000. Shrub invasions of North American semiarid grasslands. Annu. Rev. Ecol. Syst. 31, 197–215.

Wagle, P., Kakani, V.G., 2014. Growing season variability in evapotranspiration, ecosystem water use efficiency, and energy partitioning in switchgrass. Ecohydrology 7 (1), 64–72.

Weltz, M.A., Jolley, L., Goodrich, D., Boykin, K., Nearing, M., Stone, J., Guertin, P., Hernandez, M., Spaeth, K., Pierson, F., Morris, C., Kepner, B., 2011. Techniques for assessing the environmental outcomes of conservation practices applied to rangeland watersheds. J. Soil Water Conserv. 66 (5), 154A–162A.

Xu, X., Niu, S., Sherry, R.A., Zhou, X., Zhou, J., Luo, Y., 2012. Interannual variability in responses of belowground net primary productivity (NPP) and NPP partitioning to long-term warming and clipping in a tallgrass prairie. Glob Change Biol. 18, 1648–1656. https://doi.org/10.1111/j.1365-2486.2012.02651.x.

Yamanaka, T., Yonetani, T., 1999. Dynamics of the evaporation zone in dry sandy soils. J. Hydrol. 217 (1), 135–148. https://doi.org/10.1016/S0022-1694(99)00021-9.

Yang, Q., Zhang, X., 2016. Improving SWAT for simulating water and carbon fluxes of forest ecosystems. Sci. Total Environ. 569–570, 1478–1488.

Yepez, E.A., Huxman, T.E., Ignace, D.D., English, N.B., Weltzin, J.F., Castellanos, A.E., Williams, D.G., 2005. Dynamics of transpiration and evaporation following a moisture pulse in semiarid grassland: A chamber-based isotope method for partitioning flux components. Agric. For. Meteorol. 132 (3), 359–376.

Zhang, X., Srinivasan, R., Hao, F., 2007. Predicting hydrologic response to climate change in the Luohe River basin using the SWAT model. Trans. ASABE 50 (3), 901–910.

Zhang, Y., Zhang, L., Hou, J.L., Gu, J., Huang, C.L., 2017. Development of an evapotranspiration data assimilation technique for streamflow estimates: a case study in a semi-arid region. Sustainability 9.

Zhao, M., Running, S.W., 2010. Drought-induced reduction in global terrestrial net primary production from 2000 through 2009. Science 329 (5994), 940–943.

Zhao, M., Heinsch, F.A., Nemani, R.R., Running, S.W., 2005. Improvements of the MODIS terrestrial gross and net primary production global data set. Remote Sens. Environ. 95 (2), 164–176.

Zou, C.B., Turton, D.J., Will, R.E., Engle, D.M., Fuhlendorf, S.D., 2014. Alteration of hydrological processes and streamflow with juniper (Juniperus virginiana) encroachment in a mesic grassland catchment. Hydrol. Process. 28 (26), 6173–6182.

Zou, C.B., Qiao, L., Wilcox, B.P., 2015. Woodland expansion in central Oklahoma will significantly reduce streamflows - a modelling analysis. Ecohydrology 9 (5), 807–816.

Zou, C.B., Lambert, L.H., Everett, J., Will, R.E., 2022. Response of surface runoff and sediment to converting a marginal grassland to a switchgrass (*Panicum virgatum*) bio-energy feedstock system. Land 11 (4), 540.